Inadequate lung development and bronchial hyperplasia in mice with a targeted deletion in the *Dutt1/Robo1* gene

Jian Xian*, Katherine J. Clark*, Rosalyn Fordham*, Richard Pannell†, Terence H. Rabbitts†, and Pamela H. Rabbitts*‡

*Medical Research Council (MRC) Molecular Oncology Group, Department of Oncology, University of Cambridge, MRC Centre, and †MRC Laboratory of Molecular Biology, Hills Road, Cambridge CB2 2QH, United Kingdom

Edited by George Klein, Karolinska Institute, Stockholm, Sweden, and approved October 10, 2001 (received for review August 2, 2001)

Chromosome 3 allele loss in preinvasive bronchial abnormalities and carcinogen-exposed, histologically normal bronchial epithelium indicates that it is an early, possibly the first, somatic genetic change in lung tumor development. Candidate tumor suppressor genes have been isolated from within distinct 3p regions implicated by heterozygous and homozygous allele loss. We have proposed that *DUTT1,* nested within homozygously deleted regions at 3p12–13, is the tumor suppressor gene that deletion-mapping and tumor suppression assays indicate is located in proximal 3p. The same gene, *ROBO1* (accession number AF040990), was independently isolated as the human homologue of the *Drosophila* gene, *Roundabout*. The gene, coding for a receptor with a domain structure of the neural-cell adhesion molecule family, is widely expressed and has been implicated in the guidance and migration of axons, myoblasts, and leukocytes in vertebrates. A deleted form of the gene, which mimics a naturally occurring, tumor-associated human homozygous deletion of exon 2 of *DUTT1/ROBO1*, was introduced into the mouse germ line. Mice homozygous for this targeted mutation, which eliminates the first Ig domain of Dutt1/Robo1, frequently die at birth of respiratory failure because of delayed lung maturation. Lungs from these mice have reduced air spaces and increased mesenchyme, features that are present some days before birth. Survivors acquire extensive bronchial epithelial abnormalities including hyperplasia, providing evidence of a functional relationship between a 3p gene and the development of bronchial abnormalities associated with early lung cancer.

The chromosomal location of tumor suppressor genes (TSGs) has often been first indicated by tumor-associated deletion and loss of heterozygous alleles. The successful identification of these genes has frequently relied on the isolation of candidate TSG from within much smaller homozygously deleted regions, mapping within the larger region of allele loss (1). The isolation on chromosome 3 of TSG involved in lung cancer should be ideally suited to this approach, because deletions and heterozygous loss on the short-arm chromosome 3 occur frequently in this disease. Various deletion-mapping studies have indicated that several distinct regions are involved, including a recent extensive study of 151 lung tumor biopsies and cell lines with 28 markers of polymorphic loci (2). Furthermore, homozygous deletions have been relatively easy to identify because of the large number of well characterized lung tumor cell lines (3). By using fluorescence *in situ* hybridization, homozygous deletions at 3p12, 3p14, and 3p21 have been shown also to exist in biopsy material (4).

Despite thorough investigation of genes within these homozygous deletions, none has emerged as a "classic" TSG with allele loss surrounding the gene on one chromosome and point mutations in the gene in the remaining homologue. However, it is becoming increasingly recognized that TSGs may be inactivated by epigenetic mechanisms (5). Several genes on chromosome 3 fall into this category. Isoforms of the *123F2/RASSF1* gene and the *FHIT* gene are particularly noteworthy, because both have reduced or aberrant expression in lung (and other) tumors and have suppressed tumorigenicity after transfection into tumor cell lines (6, 7). Inactivation of the *Fhit* gene in mice results in gastric and sebaceous gland tumor formation in mutant mice challenged intragastrically with carcinogen (8).

We have described a large homozygous deletion at 3p12–13 in a small cell lung cancer line, U2020. After construction of a physical map of this region, CpG island mapping was used to identify gene location (9). One such gene, named *DUTT1* (accession number Z95708; deleted in U2020), mapped within smaller homozygous deletions in two other tumor cell lines (9). The smallest deletion is within the gene itself, removing a single exon (exon 2), implying that *DUTT1* might be the TSG that deletion-mapping (2, 10) and tumor suppression assays (11) indicate is located in proximal 3p. The same gene, *ROBO1*, was independently isolated as the human homologue of the *Drosophila* gene, *Roundabout*, involved in axonal guidance and midline crossing control (12). The *DUTT1/ROBO1* gene is widely expressed in mammals and codes for a receptor with a domain structure of the NCAM family (13). Members of the Slit family are likely to be the ligands for mammalian Robo (14). Slit proteins have been expressed in lung at levels equal to or greater than in adult rat brain (15).

Like other candidate TSGs on 3p, *DUTT1/ROBO1* does not show evidence of a high frequency of somatic point mutations in lung tumors (P.H.R., unpublished observations). To determine whether *DUTT1/ROBO1* has a role in lung cancer development, a deleted form of the gene was introduced into the mouse germ line, mimicking the structure of a naturally occurring human homozygous deletion of exon 2 detected in a small cell lung cancer cell line, NIH-H219X (9). Mice homozygous for the targeted mutation, which eliminates the first Ig domain of Dutt1/Robo1, frequently die at birth of respiratory failure with accompanying abnormal lung histology. Surviving mice develop bronchial hyperplasia. These studies show a functional association between the *DUTT1/ROBO1* gene and abnormal lung pathology during both fetal development and adult life.

Materials and Methods

DNA Sequencing and Contig Assembly of Mouse *Dutt1/Robo1* cDNA Clones. A mouse brain cDNA library, purchased from Stratagene, and a mouse 13.5-day embryo cDNA library, purchased from Life Technologies (Grand Island, NY), were screened with human *DUTT1/ROBO1* cDNA clones. Positive cDNA clones were sequenced and overlapped to generate a contig map that

This paper was submitted directly (Track II) to the PNAS office.

Abbreviations: TSG, tumor suppressor gene; ES, embryonic stem; H&E, hematoxylin/eosin.

See commentary on page 14763.

‡To whom reprint requests should be addressed. E-mail: phr@mrc-lmb.cam.ac.uk.

The publication costs of this article were defrayed in part by page charge payment. This article must therefore be hereby marked "*advertisement*" in accordance with 18 U.S.C. §1734 solely to indicate this fact.

was entered into the GenBank database. All sequencing reactions were performed by the Sanger dideoxy chain termination method with the Sequenase version 2 kit (United States Biochemical). The sequence of the cDNA clones was independently confirmed (Oswell Research Products Ltd., Lab 5005, Southampton, U.K.).

Generation of *Dutt1*/*Robo1*$^{-/-}$ Mice. A genomic library of E14 TG2a embryonic stem (ES) cell DNA cloned in λ2001 was screened with a mouse *Dutt1*/*Robo1* cDNA clone corresponding to exon 2 and positive clones purified and subcloned. An 8.0-kb *Sac*I fragment containing exon 2 of the mouse *Dutt1*/*Robo1* gene was used for construction of the targeting vector. A neomycin expression cassette (16) [pMC1-neomycin poly(A)] corrected to the wild-type neomycin sequence (17), was used to replace a 0.7-kb genomic *Hin*dIII, *Bam*HI fragment spanning sequences coding for exon 2 of the *Dutt1* gene (accession number Y17793). The replacement sequence was flanked 5′ by 4.4 kb and 3′ by 1.4 kb of genomic sequence. A thymidine kinase gene expression cassette (18) was ligated to a unique *Xba*I site at the 5′ end of the longer homologous arm. The final vector was linearized with *Hin*dIII for electroporation. CCB ES cells were maintained on mouse embryonic feeders. Twenty-five micrograms of *Hin*dIII-digested targeting vector DNA were used to electroporate 1×10^7 CCB ES cells. *Sac*I-digested genomic DNA from cell clones surviving G418 (GIBCO) at 400 μg/ml, and Gancyclovir at 2.5 μM selection was subjected to Southern blot analysis. Positively targeted clones were confirmed by using a 5′ end 0.7-kb *Bam*HI fragment internal probe and a 0.4-kb *Hin*dIII/*Sac*I probe external to the homologous sequence on genomic DNA digested with *Sac*I. ES cells from two independent clones were used for injection into blastocysts derived from C57BL/6 mice. Blastocysts were transferred to pseudopregnant females, and chimeric offspring were detected by the presence of agouti color on a nonagouti background. Chimeric males were mated to C57BL/6 females to produce ES cell-derived offspring. Their genotype was confirmed by Southern blot analysis of tail DNA. Mice heterozygous for the gene-targeting event—i.e., with a deletion of exon 2 of the *Dutt1*/*Robo1* gene—were intercrossed to generate homozygotes.

RNA Analysis. Total RNA was prepared from various tissues with Trizol Reagent (GIBCO/BRL). Reverse transcription (RT) reactions were performed on total RNA (5 μg) in 20 μl containing 0.5 μg of random hexamer (Amersham Pharmacia), 25 mM Tris·HCl (pH 8.3), 50 mM KCl, 2.0 mM DTT, 5.0 mM $MgCl_2$, 1 mM each of dATP, dCTP, dGTP, and dTTP, 1 unit/μl of RNasin ribonuclease inhibitor (Promega), and 10 units/μg of SUPER RT (HT Biotechnology Ltd., Cambridge, England). Each RT reaction was at 42°C for 40 min. The product of RT was diluted 5-fold and amplified by PCR (30 cycles of 1-min denaturation at 95°C, 1-min annealing at 55°C, and 1-min extension at 72°C). The following primers used were: exon 1 forward 5′-AGGGATTGACAAGCCTCCGG-3′, exon 2 reverse 5′-AGCTACCTCCAGCGATGCGT-3′, exon 3 reverse 5′-CATCTTTATCATCCAGGGGT-3′. The products were visualized after electrophoresis on agarose gels.

Western Blotting. Protein lysates were prepared with a lysis buffer composed of 9 M urea, 75 mM Tris·HCl (pH 7.5), and 0.15 M β-mercaptoethanol as described (19). Protein concentration was determined by using the Bradford assay (Bio-Rad). For Western blotting, 50 μg of protein lysate was subjected to SDS/PAGE on a 10% polyacrylamide gel and transferred onto a nitrocellulose membrane (BioTrace from Gelman). Transfer was assessed by Ponceau S staining (Bio-Rad). Filters were incubated with a polyclonal antisera raised against the C-terminal peptide of DUTT1/ROBO1 (CYERGEDNNEELEETES) followed by horseradish peroxidase-conjugated mouse anti-rabbit IgG and visualized by enhanced chemiluminscence (Amersham Pharmacia).

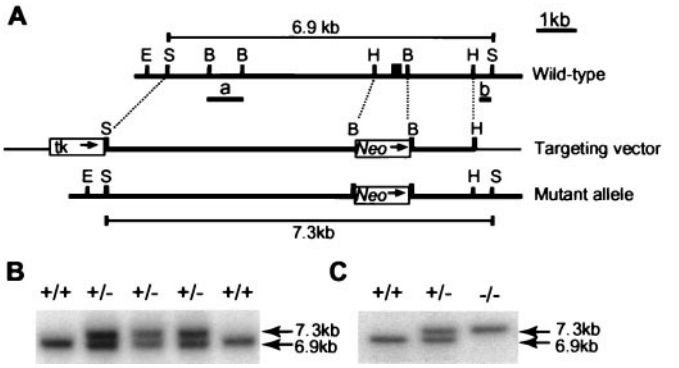

Fig. 1. Targeted mutation of the *Dutt1*/*Robo1* gene. (*A*) The genomic structure of the targeted locus and the targeting construct and mutant allele. The filled box represents exon 2. Fragments a and b are the hybridization probes used in *B*. The outer dashed lines indicate the fragment used for homologous recombination. E, *Eco*RI; S, *Sac*I; B, *Bam*HI. (*B*) After transfection of the targeting construct into ES cells, *Sac*I-digested DNA was prepared from G418-resistant ES (+/−) and control ES cells (+/+) and analyzed by Southern blot analysis The filter was hybridized to probe a which flanks the site of homologous recombination at the 3′ end, and with probe b external to the homologous integration, not shown. Two clones showing correct homologous recombination (i.e., both wild-type, 6.9-kb, and mutant, 7.3-kb alleles) were injected into blastocysts; the resulting chimeras were bred with C57BL/6 mice to obtain transmission of the mutant allele in the germ line (results not shown). (*C*) Finally mice with germ-line transmission, *Dutt1*/*Robo1*$^{+/-}$, were intercrossed to obtain offspring that were homozygous (−/−) for the targeted mutation. *Sac*I-digested tail DNA from offspring from this intercross was screened by Southern blotting with probe a.

Histological Analysis and Immunohistochemistry. Tissues or whole embryos were fixed in 4% paraformaldehyde in PBS buffer for at least 24 h, paraffin embedded, and processed to give 5-mm sections. Sections were stained with hematoxylin/eosin (H&E). For immunohistochemistry, Dutt1/Robo1 was detected by using the polyclonal antisera described above followed by donkey biotin-conjugated anti-rabbit secondary antibody and Cy-3-conjugated Streptavidin. Slides were mounted with a Vectashield-mounting medium.

Results

Generation of *Dutt1*/*Robo1* Mutant Mice. The *Dutt1*/*Robo1* gene was disrupted in mice by targeted replacement of exon 2 with the neomycin phosphotransferase gene, producing a mutant form of the gene unable to code for the first Ig domain (Fig. 1*A*), exactly reproducing a truncated *DUTT1*/*ROBO1* transcript detected in the human lung cancer cell line NIH-H219X (9). After transfection, DNA from G418-resistant ES cell clones was analyzed by Southern blotting to identify correctly targeted clones by hybridization with probe a within the targeting construct (Fig. 1*B*) and with probe b external to the homologous integration. Two such clones were injected into blastocysts and resulting chimeras bred with C57BL/6 mice. Tail DNA from offspring was screened by Southern blotting to identify mice carrying the mutant form of the gene in their germ line (Fig. 1*C*). Heterozygotes were interbred to produce homozygous offspring. Reverse transcription PCR was used to confirm that exon 1 and 3 sequences were contiguous and that exon 2 was absent in the transcript from *Dutt1*/*Robo1*$^{-/-}$ mice (data not shown).

Dutt1/Robo1 Protein in Mutant and Normal Mice. In all organs from homozygous offspring examined by Western blotting (embryos and newborn mice), the resulting protein is shorter by 20 kDa

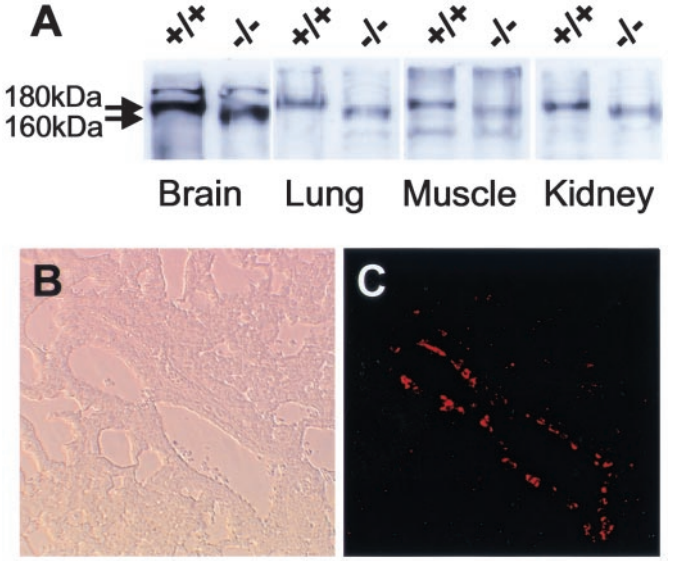

Fig. 2. Dutt1/Robo1 protein analysis (24). (*A*) Western blot analysis of protein isolated from the organs shown from wild-type (+/+) and *Dutt1/Robo1*$^{-/-}$ (−/−) day 15 embryos by using antiserum raised against a C-terminal DUTT1/ROBO1 peptide. (*B*) Phase-contrast image of a 4-μm transverse section of paraformaldehyde-fixed normal newborn lung (×200 magnification). (*C*) Detection by immunohistochemistry of Dutt1/Robo1 protein by using antipeptide antiserum in *A* in bronchial epithelium with a Cy-3-TSA amplification system (NEN Life Sciences) applied to the same section as in *B* (×200 magnification).

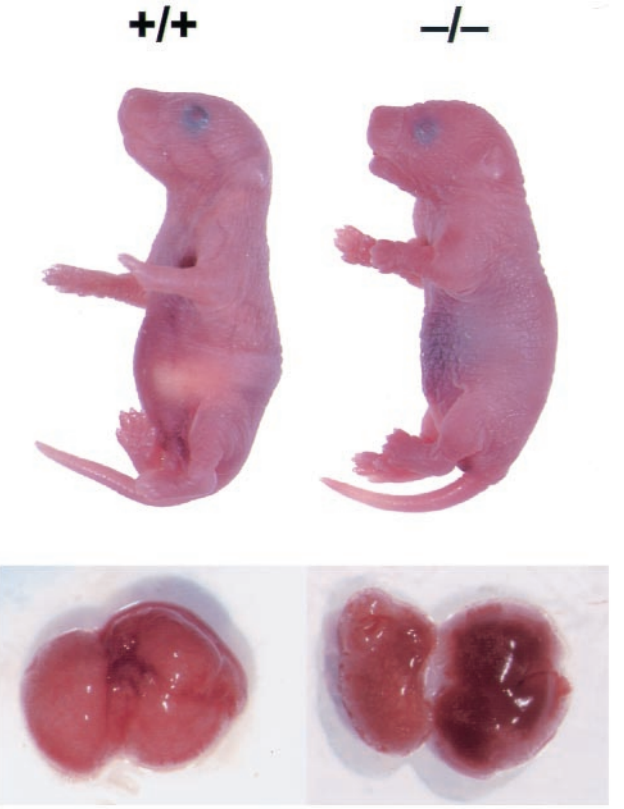

Fig. 3. Gross morphological phenotypes of wild-type and *Dutt1/Robo1*$^{-/-}$ mice. A wild-type mouse and its lungs shown below (+/+) compared with a *Dutt1/Robo1*$^{-/-}$ mouse and its lungs shown below (−/−).

because of loss of the first Ig domain encoded by exon 2 (Fig. 2*A*). Densitometry of Western blotting indicated that levels of the Dutt1/Robo1 mutant protein in E15 mice were reduced to 80% in brain and 45% in lung compared with wild-type protein.

Immunohistochemistry was performed with a polyclonal antibody raised against the C terminus of human DUTT1/ROBO1 (K.J.C., J.X., E.H., and P.H.R., unpublished observations), which recognizes the mouse protein. This procedure detected the protein at high levels in epithelial cells lining bronchi but at low or undetectable levels in adjacent mesenchyme and cells lining alveoli (Fig. 2*B*).

***Dutt1/Robo1*$^{-/-}$ Mice Frequently Die at Birth Because of Respiratory Failure.** Mice heterozygous for the *Dutt1/Robo1* deletion were born at the expected frequency and had no obviously abnormal phenotype. At birth, *Dutt1/Robo1*$^{-/-}$ mice failed to feed (Fig. 3) and were usually inactive with labored breathing; 38 of 50 (63%) died within the first 24 h. At autopsy, lungs were frequently dark red (Fig. 3) and sank in fixative, which suggests inadequate inflation. After fixation and H&E staining, lungs from *Dutt1/Robo1*$^{-/-}$ mice and their normal littermates were compared. The most striking feature of lungs from *Dutt1/Robo1*$^{-/-}$ newborn mice was increased cellularity of the mesenchyme resulting in reduction of the size of terminal air spaces (Fig. 4*D*); alveolar septa were reduced in number and thicker than in the wild-type littermates (Fig. 4*C*); the bronchioles were of an irregular cross section (Fig. 4*D*). The overall appearance was consistent with a developmental delay of 0.5–1.0 day. To determine whether the abnormal phenotypes were present before birth, lungs from day E15.5 and day E18.5 were similarly examined. This showed that the abnormal lung morphology was already established at day E15.5 (Fig. 4 *A* and *B*).

Search for Other Phenotypic Changes in *Dutt1/Robo1*$^{-/-}$ Mice. All newborn mice that died at birth were examined for macroscopic abnormalities in addition to their abnormal lungs. None was found except that three mice had diaphragmatic hernias. The heart, kidneys, and muscle were examined microscopically, but no abnormal histology was detected. In view of the function of Drosophila Robo in the control of axonal migration and the high level of expression of the protein in the brain of newborn mice (Fig. 2*A*) and in fetal brain (K.J.C., J.X., E. Hammond, and P.H.R., unpublished observations), brains and spinal cords of mutant mice were examined. Transverse serial sections of spinal cord from E12.5 and E15.5 embryos were examined by H&E staining for thickening of the ventral commissures underlying the floor plate of the spinal chord. However, no differences could be detected between *Dutt1/Robo1*$^{-/-}$ and normal embryos (data not shown).

Development of Bronchial Epithelial Hyperplasia in *Dutt1/Robo1*$^{-/-}$ Mice Surviving Birth. Our results show that the *Dutt1/Robo*-targeted germ-line mutation, which emulated the naturally occurring somatic mutation found in the NCIH219X lung tumor cell line, has a profound effect on lung development. Some homozygous mice do survive to adulthood and are capable of breeding (37%). The *Dutt1/Robo1*$^{-/-}$ mice surviving beyond the first 24 h after birth seemed to develop normally, but 15 of 22 mice have so far shown signs of morbidity at ages ranging from 3 weeks to 13 months. After autopsy and tissue examination of all major organs, bronchial epithelial hyperplasia was observed in 9 of 10 mice examined but with no obvious increase in the extent of abnormalities with age. In six of nine sets of serial lung sections cut at different levels, papillary hyperplasia was seen throughout the entire bronchial tree (Fig. 4 *F* and *H*), contrasting with the uniform cuboidal appearance of the bronchial epithelium of normal adult mice (Fig. 4 *E* and *G*). In the remaining three sets, hyperplasia was seen in individual lobes. In three of

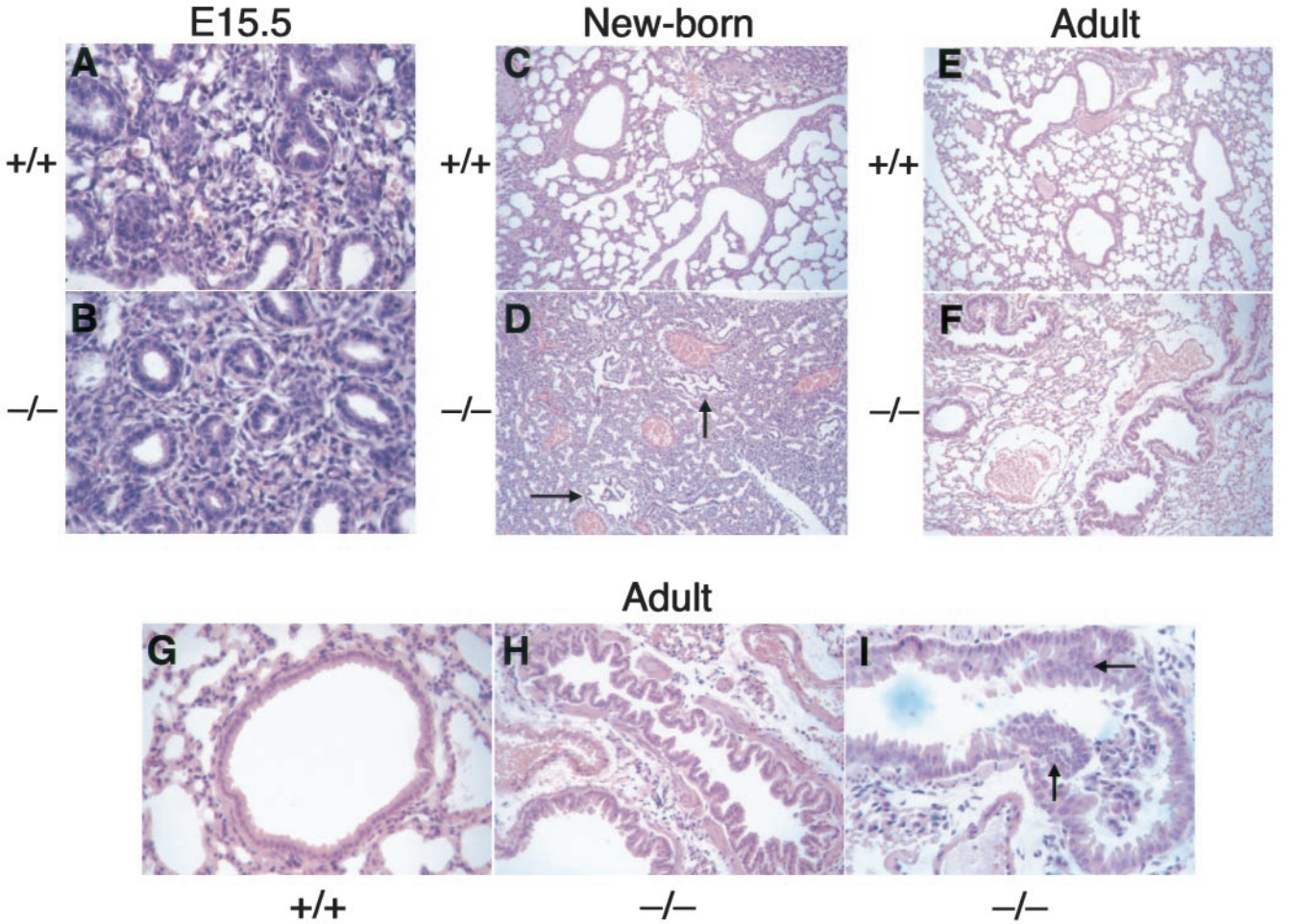

Fig. 4. Histological analysis of lungs of *Dutt1*/*Robo1*$^{-/-}$ mice and wild-type littermates. Paraformaldehyde-fixed 4-μm sections of lung tissue were H&E-stained and photographed. (*A*) Wild-type lung, embryo day E15.5 (×400 magnification); (*B*) *Dutt1*/*Robo1*$^{-/-}$ lung, embryo day 15.5 (×400 magnification); (*C*) wild-type newborn lung (×100 magnification); (*D*) *Dutt1*/*Robo1*$^{-/-}$ newborn lung (×100 magnification; arrow indicates bronchi); (*E*) wild-type adult lung (×100 magnification); (*F*) *Dutt1*/*Robo1*$^{-/-}$ adult lung (×100 magnification); (*G*) wild-type adult lung (×400 magnification); (*H*) *Dutt1*/*Robo1*$^{-/-}$ adult lung (×400 magnification); (*I*) *Dutt1*/*Robo1*$^{-/-}$ adult lung (×400 magnification; focal dysplasia indicated by arrow). Populations of mice were established from two independent ES clones; both gave indistinguishable abnormal lung pathology.

the sets of serial sections from mice with full involvement of the bronchial tree, focal dysplasia was observed. The focal dysplasia was characterized by increased epithelial cell layers, large pleomorphic nuclei, and reduced cytoplasm (Fig. 4*I*). Thus, although differences in gross lung morphology are less distinct in surviving postnatal homozygotes, specific bronchial epithelial alterations are apparent in these mice.

Discussion

Positional cloning, the identification of a gene by its chromosomal location, has been effective in identifying several genes involved in cancer development. However, after initial isolation, their function is unknown and these genes are considered candidate oncogenes or TSGs until evidence accrues that confirms their proposed involvement in tumorigenesis. For TSGs, the development of a tumor-related phenotype in mice in which the orthologue of the candidate gene has been inactivated by gene targeting provides strong support for the involvement of the candidate gene in tumor development (20). By using this approach with the *DUTT1*/*ROBO1* gene, we have generated mice with abnormal bronchial epithelial phenotypes, strengthening our previous suggestion that this gene is involved in lung tumor development (9).

The *Dutt1*/*Robo1*$^{-/-}$ mice created in these experiments carry an altered form of the gene in which deletion of exon 2 has resulted in a truncated protein devoid of the first Ig domain. Although not a complete null, it seems likely that this mutant allele results in loss of function for the following reasons. Although the effect of the loss of the first Ig domain (coded for by exon 2) on the activity of Dutt1/Robo1 as a receptor is unknown, this domain is the most conserved within this family of proteins (12); its removal, therefore, may be expected to have a pronounced effect on protein function. Determination of the structure of the first four Ig domains of Axonin-1/TAG-1, a protein with a very similar domain structure, supports this prediction because they are arranged in a U shape with contacts between Ig domains 1 and 4 (21). Although the ligand(s) of epithelial Dutt1/Robo1 are unknown, Slit2 and -3 are strong candidates (14). In axonal guidance and neuronal migration in *Xenopus*, the Robo Ig domains alone are sufficient for signaling through Slit2 (22). Structure/function studies of Dutt1/Robo1 and its ligand(s) in epithelial signaling will help to clarify the roles of the various domains. The most compelling evidence for a loss-of-function phenotype is provided by the requirement for loss of both alleles for manifestation of the abnormal lung phenotypes. It is possible that the loss-of-function effect is

incomplete and has different penetration in different tissues, perhaps because of the involvement of different ligands, explaining the substantial effect on lung maturation compared with axonal guidance. The phenotype of mutant mice with complete ablation of the *Dutt1/Robo1* gene will address this issue.

The *Dutt1/Robo*$^{-/-}$ mice that die shortly after birth have observable respiratory failure and lungs with macroscopic and microscopic abnormalities. Two approaches were used to determine whether these abnormalities were caused by a primary defect of lung development or were a secondary consequence of a deficiency in the neuronal network. Because Robo$^{-/-}$ mutants in *Drosophila* show defects of midline crossing (12), we compared *Dutt1/Robo1*$^{-/-}$ and normal mouse embryos for thickening of the ventral commissures underlying the floor plate of the spinal cord by using H&E staining. No obvious differences could be detected (data not shown), although these may be revealed by more detailed analysis. Direct evidence for primary involvement of the *Dutt1/Robo1* gene in lung development was provided by examination of lung morphology during fetal development. By day E15.5, the abnormal lung morphology was already established; lungs of *Dutt1/Robo1*$^{-/-}$ embryos showed denser packing of lung mesenchyme than wild-type controls (Fig. 4 *A* and *B*). The normal pattern of expression of Dutt1/Robo1 within newborn lungs is consistent with a primary rather than a secondary defect in lung, because antibody to the protein detects Dutt1/Robo1 expression specifically in bronchial epithelium (Fig. 2*B*). The observations reported here demonstrate an association between a chromosome 3 candidate TSG and abnormal lung development. Not enough is known about the function of the Robo/Slit family in epithelial–mesenchymal interactions to provide a mechanistic explanation for the link between the underlying genetic defect and the observed phenotype.

Most *Dutt1/Robo1*$^{-/-}$ mice surviving birth develop signs of morbidity by 1 year of age and have abnormal bronchial structures as the common and often the only observable abnormality. The atypical histology is most pronounced in the epithelial layer, in particular the major airways of the lung corresponding to where the Dutt1/Robo1 protein shows specific expression in newborn (Fig. 2*B*) and adult lungs (data not shown). The observed cellular phenotypes of hyperplasia and dysplasia have a parallel in the early development of human lung cancer (23). Null mutations of the *Drosophila Robo* gene result in failure of commissural axons to respond to guidance cues causing their aberrant migration (12). Recently, Slit–Robo interactions have been involved in inhibition of leukocyte migration (15). Knowledge of a gene's normal and pathological function in one species or tissue may enable prediction of its behavior in another. Thus, the mammalian orthologue may perform a related function in epithelial cells. The abnormal lung phenotypes reported here may reflect a similar failure in cells to maintain their correct position, perhaps because of uncontrolled cell migrations, resulting in the observed aberrations in tissue architecture in lungs of newborn and adult mice.

Tumor formation is believed to require sequential somatic genetic changes that drive the progressive morphological abnormalities toward the fully malignant phenotype (24). For lung cancer, deletions of chromosome 3 are frequent (2), and regions of homozygous loss on 3p (2, 4) are associated with candidate TSGs. Somatic damage to 3p is believed to be one of the earliest events in lung tumor formation because hemizygous loss of 3p alleles correlates with the emergence and development of preinvasive lesions including hyperplasia (25, 26). Additional genetic changes are required for full malignancy (25). Thus, the observation of bronchial epithelial hyperplasia, but no tumor formation, in these mutant mice with a defective 3p orthologue is the phenotype anticipated from a knowledge of the initiation of human lung cancer and its associated somatic genetic changes. Further genetic damage to these mutant mice, either by clastogenic agents or directed to other loci involved in the development of human lung tumors, may result in progression toward a more malignant phenotype. These *Dutt1/Robo1* mutants would then be a useful starting point for the construction of mouse models of multistep lung tumor development driven by the sequential somatic genetic changes known to be involved in human lung cancer.

We thank James Greenberg, Linda Bobrow, Francesco Pezzella, and Padriac Fallon for help with lung histopathology, Mau-Ching Wu for *Dutt1/Robo1* cDNA clones, and Grace Chung and Vasi Sundaresan for unpublished details of *DUTT1/ROBO1* gene structure. This work was supported by Grant G9703123 from the Medical Research Council. T.H.R. and R.P. are funded by a Medical Research Council grant to the Laboratory of Molecular Biology.

1. Marshall, C. J. (1991) *Cell* **64,** 313–326.
2. Wistuba, I. I., Behrens, C., Virmani, A. K., Mele, G., Milchgrub, S., Girard, L., Fondon, J. W., III, Garner, H. R., McKay, B., Latif, F., *et al*. (2000) *Cancer Res.* **60,** 1949–1960.
3. Oie, H. K., Russell, E. K., Carney, D. N. & Gazdar, A. F. (1996) *J. Cell. Biochem.* **24,** Suppl., 24–31.
4. Todd, S., Franklin, W. A., Varella-Garcia, M., Kennedy, T., Hilliker, C. E., Jr., Hahner, L., Anderson, M., Wiest, J. S., Drabkin, H. A. & Gemmill, R. M. (1997) *Cancer Res.* **57,** 1344–1352.
5. Baylin, S. B., Belinsky, S. A. & Herman, J. G. (2000) *J. Natl. Cancer Inst.* **92,** 1460–1461.
6. Dammann, R., Li, C., Yoon, J. H., Chin, P. L., Bates, S. & Pfeifer, G. P. (2000) *Nat. Genet.* **25,** 315–319.
7. Siprashvili, Z., Sozzi, G., Barnes, L. D, McCue, P., Robinson, A. K., Eryomin, V., Sard, L., Tagliabue, E., Greco, A., Fusetti, L., *et al*. (1997) *Proc. Natl. Acad. Sci. USA* **94,** 13771–13776.
8. Fong, L. Y., Fidanza, V., Zanesi, N., Lock, L. F., Siracusa, L. D., Mancini, R., Siprashvili, Z., Ottey, M., Martin, S. E., Druck, T., *et al.* (2000) *Proc. Natl. Acad. Sci. USA* **97,** 4742–4747. (First Published April 11, 2000; 10.1073/pnas.080063497)
9. Sundaresan, V., Chung, G., Heppell-Parton, A., Xiong, J., Grundy, C., Roberts, I., James, L., Cahn, A., Bench, A., Douglas, J., *et al.* (1998) *Oncogene* **17,** 1723–1729.
10. Daly, M. C., Douglas, J. B., Bleehen, N. M., Hastleton, P., Twentyman, P. R., Sundaresan, V., Carritt, B., Bergh, J. & Rabbitts, P. H. (1991) *Genomics* **9,** 113–119.
11. Lott, S. T., Lovell, M., Naylor, S. L. & Killary, A. M. (1998) *Cancer Res.* **58,** 3533–3537.
12. Kidd, T., Brose, K., Mitchell, K. J., Fetter, R. D., Tessier-Lavigne, M., Goodman, C. S. & Tear, G. (1998) *Cell* **92,** 205–215.
13. Sundaresan, V., Roberts, I., Bateman, A., Bankier, A., Sheppard, M., Hobbs, C., Xiong, J., Minna, J., Latif, F., Lerman, M. & Rabbitts, P. (1998) *Mol. Cell. Neurosci.* **11,** 29–35.
14. Piper, M., Georgas, K., Yamada, T. & Little, M. (2000) *Mech. Dev.* **94,** 213–217.
15. Wu, J. Y., Feng, L., Park, H. T., Havlioglu, N., Wen, L., Tang, H., Bacon, K. B., Jiang, Z., Zhang, X. & Rao, Y. (2001) *Nature (London)* **410,** 948–952.
16. Thomas, K. R. & Capecchi, M. R. (1987) *Cell* **51,** 503–512.
17. Yenofsky, R. L., Fine, M. & Pellow, J. W. (1990) *Proc. Natl. Acad. Sci. USA* **87,** 3435–3439.
18. Mansour, S. L., Thomas, K. R. & Capecchi, M. R. (1988) *Nature (London)* **336,** 348–352.
19. Schmeiser, K., Hammond, E. M., Roberts, S. & Grand, R. J. (1998) *FEBS Lett.* **433,** 51–57.
20. Zhu, Y., Richardson, J. A., Parada, L. F. & Graff, J. M. (1998) *Cell* **94,** 703–714.
21. Freigang, J., Proba, K., Leder, L., Diederichs, K., Sonderegger, P. & Welte, W. (2000) *Cell* **101,** 425–433.
22. Chen, J. H., Wen, L., Dupuis, S., Wu, J. Y. & Rao, Y. (2001) *J. Neurosci.* **21,** 1548–1556.
23. McDowell, E. M. & Beals, T. F. (1986) *Biopsy Pathology of the Bronchi* (Chapman & Hall, New York).
24. Vogelstein, B. & Kinzler, K. W. (1993) *Trends Genet.* **9,** 138–141.
25. Chung, G. T., Sundaresan, V., Hasleton, P., Rudd, R., Taylor, R. & Rabbitts, P. H. (1995) *Oncogene* **11,** 2591–2598.
26. Hung, J., Kishimoto, Y., Sugio, K., Virmani, A., McIntire, D. D., Minna, J. D. & Gazdar, A. F. (1995) *J. Am. Med. Assoc.* **273,** 1908.